Liquid Crystalline Polyethers and Copolyethers Based on Conformational Isomerism. 3. The Influence of Thermal History on the Phase Transitions of Thermotropic Polyethers and Copolyethers Based on 1-(4-Hydroxyphenyl)-2-(2-methyl-4-hydroxyphenyl)ethane and Flexible Spacers Containing an Odd Number of Methylene Units

Virgil Percec* and Raymond Yourd

Department of Macromolecular Science, Case Western Reserve University, Cleveland, Ohio 44106. *Received November 14, 1988; Revised Manuscript Received January 24, 1989*

ABSTRACT: The influence of thermal history on the phase transitions of thermotropic polyethers (MBPE-5, MBPE-7, MBPE-9, and MBPE-11) and copolyethers (MBPE-*X*/*Y*; *X*, *Y* = 5, 7, 9, 11) based on 1-(4-hydroxyphenyl)-2-(2-methyl-4-hydroxyphenyl)ethane (MBPE) and flexible spacers containing 5, 7, 9, and 11 methylene units is described. All polymers display two crystalline phases (one that melts at low temperatures below the nematic–isotropic transition and the other that melts at high temperatures above the nematic–isotropic transition), a smectic and a nematic mesophase. As determined from second or subsequent differential scanning calorimetry scans, the homopolymers present virtual or monotropic mesophases, while the copolymers with various compositions close to a 50/50 molar ratio of two spacers exhibit both smectic and nematic enantiotropic mesophases. Upon annealation at different temperatures, the monotropic or enantiotropic character of the mesophases is determined by the rate of crystallization of each of the two crystalline phases. The longer the spacer length(s), the higher the rate of crystallization. After annealing at room temperature, a mixture of low- and high-temperature crystalline phases is obtained for MBPE-5/7 and MBPE-5/9 copolymers, and therefore most of their enantiotropic mesophases become monotropic. The rate of crystallization of the other copolymers is higher, and therefore, after annealing at room temperature, a high content of low-temperature crystalline phase is formed. As a consequence, the formation of the high-temperature crystalline phase is suppressed to the extent that most of the copolymers maintain their enantiotropic mesophases. Annealing at high temperatures induces the high-temperature crystalline phases in all polymers with the exception of MBPE-7/9(50/50) and MBPE-7/9(60/40). Therefore, under equilibrium conditions, only the MBPE-7/9(50/50) and MBPE-7/9(60/40) copolymers display an enantiotropic nematic mesophase. Under equilibrium conditions, the other copolymers and homopolymers display only virtual and/or monotropic mesophases. This behavior is determined by the thermodynamically controlled character of the mesophase and the kinetically controlled character of crystalline phases. Consequently, transformation of a virtual or monotropic mesophase into an enantiotropic one by copolymerization represents a kinetic effect, and at the present time, the unusual behavior of the MBPE-7/9(50/50) and MBPE-7/9(60/40) copolymers remains unexplained.

Introduction

Traditional *rigid rodlike* mesogenic units are constituted by linearly substituted aromatic or cycloaliphatic rings connected by rigid interconnecting groups which provide a linear and eventually planar conformation to the resulting compound. Although there is free rotation about certain carbon–carbon single bonds of these compounds, it is essential that rotation about these single bonds does not perturb the elongated or extended conformation of the mesogenic group. Therefore, in rigid rodlike mesogenic units, the extended conformation of the molecule is accomplished and maintained through the rigidity and linearity of its constituents, i.e., its rigid rodlike character (Scheme I).

The transplant of this concept from low molar mass liquid crystals to macromolecular liquid crystals led to the presently accepted pathway used in the synthesis of both main-chain and side-chain liquid crystalline polymers.

An alternative solution to the creation of an extended conformation of a molecule can be considered when the rigid interconnecting groups from the rigid rodlike mesogens are replaced with *flexible* interconnecting units, as, for example, ethylene or methyleneoxy. Although ethylene or methyleneoxy units can adopt an extended conformation which is similar to the trans one provided by an ester or trans-1,2-disubstituted vinylene units (Scheme I), these flexible interconnecting groups undergo free rotation leading to a number of different conformational isomers which are in dynamic equilibrium. Usually the two most stable conformational isomers are anti and gauche (Scheme I). Since the anti conformer has an extended conformation, it is expected to display liquid crystallinity. The

Scheme I
Comparison of Rigid Rodlike Mesogens and Flexible Rodlike Mesogens or Rodlike Mesogens Based on Conformational Isomerism

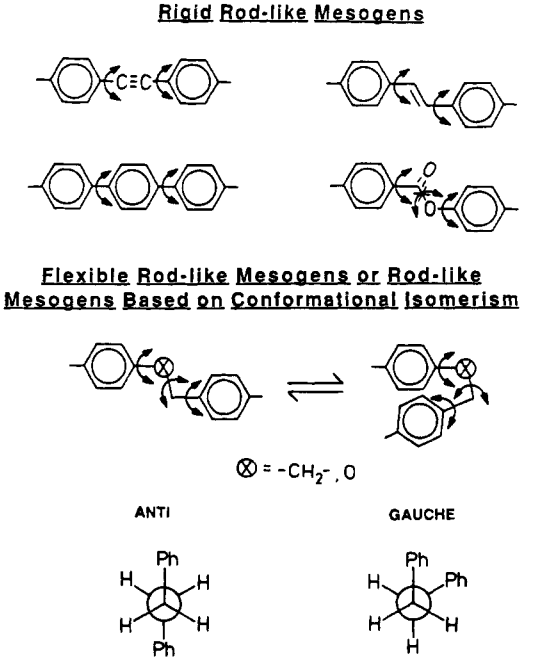

0024-9297/89/2222-3229$01.50/0

gauche conformer is similar to a "kinked" unit which is occasionally introduced within the structure of main-chain liquid crystalline copolymers to depress phase transition temperatures. The anti and gauche conformers are in dynamic equilibrium. Therefore, the insertion of flexible units capable of giving rise to extended and kinked conformers, as, for example, 1,2-diphenylethane, benzyl ether, and methyleneoxy, within the main chain of the polymer is expected to provide a liquid crystalline polymer having a dynamic composition.

In contrast to mesogenic units where the linearity and planarity of the molecule are realized and maintained through their rigid rodlike character, in the second class of mesogens, the rodlike character is realized through the conformational isomerism and maintained through the dynamic equilibrium between different conformers. Therefore, for this present class of liquid crystals or mesogenic groups, we have suggested the name *liquid crystals or rodlike mesogenic units based on conformational isomerism.*[1]

The literature on low molar mass flexible liquid crystals was briefly mentioned in the first paper from this series[1] and in more detail in a recent review.[2]

The first examples of liquid crystal polymers containing rodlike mesogenic units based on conformational isomerism belong to the class of thermotropic side-chain liquid crystalline polymers and were reported from our laboratory.[3-5] Recently, we reported the first examples of main-chain liquid crystalline polymers containing mesogenic units based on conformational isomerism.[1,6] They were prepared both as quasi-rigid polyethers (i.e., polyethers without flexible spacers)[1] and as semiflexible polyethers containing mesogenic units based on conformational isomerism and flexible spacers.[6] The examples of semiflexible main-chain polyethers and copolyethers described in the previous publication from this series are based on 1-(4-hydroxyphenyl)-2-(2-methyl-4-hydroxyphenyl)ethane (MBPE) as the flexible rodlike mesogenic unit or rodlike mesogenic unit based on conformational isomerism and flexible spacers containing 5, 7, 9, and 11 methylene units. The phase behavior of these polymers and copolymers was determined by using a combination of differential scanning calorimetry (DSC) and thermal optical polarized microscopy. Phase transitions were perfectly reproducible when they were reported from second or subsequent heating scans. However, they differed from those obtained from the first heating scans or upon application of different thermal histories. Consequently, the previous paper[6] described the phase behavior of these polymers and copolymers as obtained from the second or subsequent heating and cooling scans.

The goal of this paper is to describe the influence of thermal history on the phase behavior of the polyethers and copolyethers based on 1-(4-hydroxyphenyl)-2-(2-methyl-4-hydroxyphenyl)ethane (MBPE) and flexible spacers containing 5, 7, 9, and 11 methylene units and to compare it with the phase behavior previously determined.[6]

Experimental Section

Synthesis of Polyethers and Copolyethers. Synthesis of polyethers and copolyethers based on 1-(4-hydroxyphenyl)-2-(2-methyl-4-hydroxyphenyl)ethane and α,ω-dibromoalkanes is outlined in Scheme II, and the experimental details concerning their synthesis, purification, and structural characterization were presented in our previous paper.[6] Both polyethers and copolyethers exhibit monomodal molecular weight distributions, are free of any oligomeric products, and present number-average molecular weights higher than 20 000. Their polydispersities are less than 2.0.[6] Over the entire manuscript, the polyethers will be designated MBPE-X where X is the number of methylene units in the spacer.

Scheme II
Synthesis of Polyethers and Copolyethers Based on 1-(4-Hydroxyphenyl)-2-(2-methyl-4-hydroxyphenyl)ethane and α,ω-Dibromoalkanes

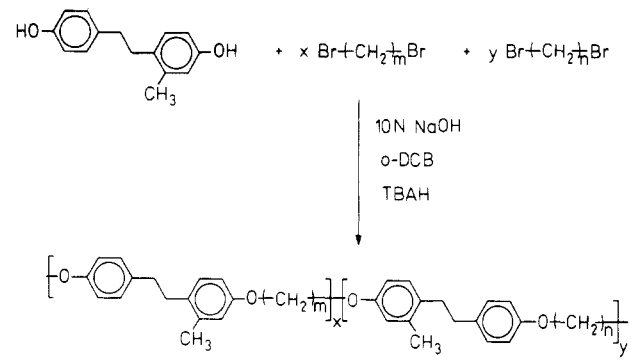

Similarly, the copolyethers will be designated MBPE-$X/Y(A/B)$ where X is the number of methylene units in one of the spacers, Y is the number of methylene units in the other spacer, and A/B refers to the molar ratio of the two spacers. Therefore, for example, MBPE-$X/Y(100/0)$ represents MBPE-X.

Techniques. A Perkin-Elmer DSC-4 differential scanning calorimeter equipped with a TADS data station model 3600 was used to determine the thermal transitions. Heating and cooling rates were 20 °C/min in all cases unless stated otherwise. First-order transitions (crystalline–crystalline, crystalline–liquid crystalline, liquid crystalline–isotropic, etc.) were read at the maximum of the endothermic or exothermic peaks. Glass transition temperatures (T_g) were read at the middle of the change in the heat capacity.

All heating and cooling DSC scans produced perfectly reproducible traces only when they were recorded after identical thermal histories. We will be concerned with four different categories of data. The first one will be only briefly mentioned since it was detailed in our previous paper;[6] it refers to thermal transitions and their corresponding thermodynamic parameters calculated from "second" or subsequent heating scans. Prior to the second heating scan, the polymer sample was heated and then cooled at 20 °C/min within the same interval of temperatures as in the second heating scan. The second series of data refer to both thermal transitions and their corresponding thermodynamic parameters determined from the "first heating scan". The first heating scan represents the first heating scan of the polymer sample as obtained after precipitation from chloroform solution into methanol followed by vacuum drying at room temperature (~25 °C) for a few days. All these polymer samples spent about 3–7 days at room temperature before the first heating scan was recorded. The third set of data refers to those collected from the "first heating scan after room-temperature annealing". This data set refers to the first heating scan determined for the same sample pan as that used for the previous two experiments. After the second and subsequent heating and cooling scans were determined, the sample pan was "annealed" at room temperature for periods of time in between 3 and 4 weeks. Then the first heating scan was recorded. In all cases, the first heating scan after room-temperature annealing is identical or almost identical with the first heating scan. Finally, the same sample pans were annealed at higher temperatures for different periods of time which are indicated on the DSC traces, and the first heating scan of the high-temperature annealed sample was recorded. Unless stated, all heating scans were recorded at 20 °C/min. While there are very significant differences between heating scans obtained for the same sample but with different thermal histories, all cooling scans are identical when recorded with the same cooling rate and they will not be discussed here since they were detailed in our previous paper.[6]

A Carl Zeiss optical polarizing microscope (magnification 200×) equipped with a Mettler FP82 hot stage and a Mettler 800 central processor was used to observe the thermal transitions and to analyze the textures.[7]

Results and Discussion

The previous paper from this series[6] describes the syn-

Table I
Characterization of Polyethers Based on MBPE and 1,5-Dibromopentane (MBPE-5) and 1,7-Dibromoheptane (MBPE-7) and of Corresponding Copolyethers [MBPE-5/7(A/B)] before and after Thermal Treatments

copolymer MBPE-5/7(A/B) 5/7 mole ratio	thermal transitions (°C) from DSC heating scans (20 °C/min) and corresponding enthalpy changes (kcal/mru) in parentheses		
	second heating scan	room-temp annealing	high-temp annealing
100/0	g 20 k 79 (1.44) k 115 (0.33) i	g 22 k 53 (0.12) k 120 (3.13) i	g 30 k 94 k 105 k 118 (3.87) i
80/20	g 19 s 51 (0.15) n 65 (0.58) i	g 20 k 48 (0.20) k 99 (2.40) i	g 20 k 99 (3.09) i
60/40	g 14 s 51 (0.15) n 64 (0.57) i	g 17 k 50 (0.07) k 60 (0.27) k 67 (0.42) i	g 15 k 64 k 81 (2.02) i
50/50	g 14 s 55 (0.16) n 68 (0.62) i	g 16 k 52 (0.25) k 63 (0.21) n 68 (0.42) i	g 14 k 79 (1.66) i
40/60	g 14 s 58 (0.13) n 70 (0.62) i	g 17 k 55 (0.37) k 72 (1.37) i	g 14 k 71 (1.47) i
20/80	g 13 k 63 (0.11) k 77 (1.55) i	g 17 k 49 (0.09) k 64 k 80 (1.81) i	g 13 k 78 (2.00) i
0/100	g 7 k 85 (2.18) i	g 11 k 45 (0.06) k 85 (2.22) i	g 9 k 85 k 99 (3.12) i

thesis and characterization of the first examples of thermotropic main-chain liquid crystalline polyethers and copolyethers based on flexible rodlike mesogenic units or rodlike mesogenic units based on conformational isomerism and flexible spacers. The particular examples presented refer to polyethers (MBPE-5, MBPE-7, MBPE-9, and MBPE-11) and copolyethers (MBPE-X/Y; X, Y = 5, 7, 9, 11) based on 1-(2-hydroxyphenyl)-2-(2-methyl-4-hydroxyphenyl)ethane (MBPE) and flexible spacers containing 5, 7, 9, and 11 methylene units. Their phase behavior was determined from the second or subsequent heating and cooling scans and can be summarized as follows. Both MBPE-5 and MBPE-9 exhibit a nematic and a smectic monotropic mesophase; MBPE-7 is crystalline, while MBPE-11 displays a monotropic nematic mesophase. However, copolymers with various compositions situated around a 50/50 molar ratio between the two spacers exhibit both nematic and smectic enantiotropic mesophases. Both liquid crystalline transition temperatures and the corresponding enthalpies of the copolymers are weight-averaged values of the similar parameters of the parent homopolymers. Extrapolation of mesomorphic transition temperatures and their enthalpy changes has demonstrated that all homopolymers exhibit virtual nematic and smectic mesophases. The thermal transition temperatures and the enthalpy changes associated with the virtual nematic and smectic mesomorphic transitions of the homopolymers were determined from several sets of copolymers with very good agreement.

One of the most important conclusions derived from these experiments seems to provide a definitive answer to one of the nonelucidated problems of semiflexible main-chain liquid crystalline copolymers, i.e., the influence of copolymer composition on mesomorphic phase transitions.[8] This conclusion is strongly supported by experimental results obtained recently in different laboratories.[9-11] It demonstrates that, within the range of molecular weights whose phase transitions are not affected by the nature of the polymer chain ends and are molecular weight independent, the liquid crystalline transitions of copolymers and their thermodynamic parameters should represent weight-averaged values of the transition temperatures and of thermodynamic parameters of the parent homopolymers. As a result of this conclusion and due to the fact that crystalline transitions are kinetically controlled while mesomorphic transitions are considered to be thermodynamically controlled, copolymerization becomes one of the most valuable tools for the identification of mesophases in liquid crystalline polymers and copolymers.

However, recently it has been shown that liquid crystalline transitions of polyethers and copolyethers based on the rigid rodlike mesogen 4,4′-dihydroxy-α-methylstilbene and flexible spacers containing an odd number of methylenic units are kinetically controlled.[15] This kinetic control almost vanishes on going to the corresponding polymers and copolymers containing an even number of methylenic units in the flexible spacer.[16] Considering also the dynamic nature of the ratio between the anti and gauche conformers of MBPE (Scheme I), we are questioning the role of thermal history of the polymer sample not only on the crystalline transitions but also on the liquid crystalline transitions of the polyethers and copolyethers based on MBPE and flexible spacers containing an odd number of methylenic units.

Without exception, the data from the literature on main-chain liquid crystalline polymers do not consider the first heating scan. This is due to its irreproducibility. Therefore, we will start our investigation by trying to understand the meaning and the reproducibility of the first heating scan. Regardless of the thermal history of the DSC scan under consideration, over the entire manuscript, the second heating scan will be plotted on the same figure with a dotted line. The new transitions occurring as a consequence of different types of annealing are shaded and therefore will be discriminated with ease from those transitions occurring in the second heating scan. The same is true if only peak size changes occur in going from second to first heating scans after annealing. For the sake of clarity, we have to mention again that discrimination between liquid crystalline and crystalline transitions of copolymers can be easily made since the former and their corresponding thermodynamic parameters represent weight-averaged values of the similar parameters of their parent homopolymers. In contrast, crystalline transitions and their thermodynamic parameters are strongly depressed by copolymerization. This is because copolymers generally display a lower rate of crystallization than the corresponding homopolymers. Therefore, only when both the thermal transition temperatures and the corresponding enthalpies of the homopolymers and copolymers, plotted as a function of composition, are situated on a straight line can they be considered to belong to a mesomorphic transition.

Parts a and b of Figure 1 present DSC traces of the second heating scans and first heating scans after room-temperature and high-temperature annealings of the polymer system MBPE-5/7. Table I summarizes the thermal transitions and thermodynamic parameters. The phase diagrams of the thermal transitions and enthalpy changes are reported in Figure 2. It is very important to realize from the very beginning that the first heating scan and first heating scan obtained after annealing at room temperature are identical within experimental error. This is an expected behavior since the glass transition temperature of all these polymers are below room temperature. Therefore, annealing at room temperature a sample which was or was not previously scanned on the DSC instrument should not produce any difference in its thermal behavior. However, first heating scans after annealing at room temperature drastically differ from second or subsequent

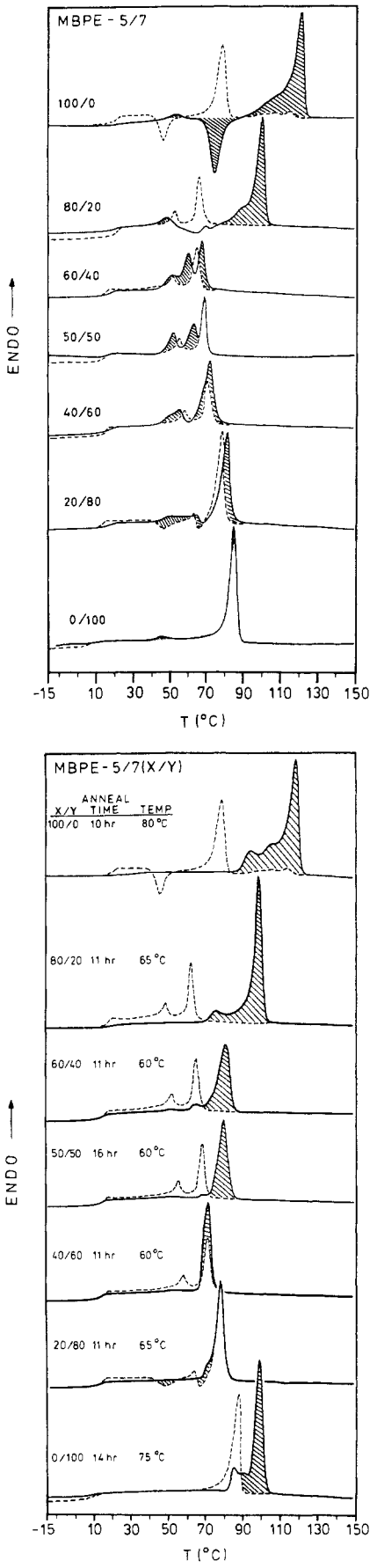

Figure 1. DSC thermograms of polyethers based on MBPE and 1,5-dibromopentane (MBPE-5), MBPE and 1,7-dibromoheptane (MBPE-7), and corresponding copolyethers [MBPE-5/7(A/B)]. (a, top) First heating scan after room-temperature annealing or first heating scan (—); second heating scan (- - -). (b, bottom) First heating scan after high-temperature annealing (—); second heating scan (- - -).

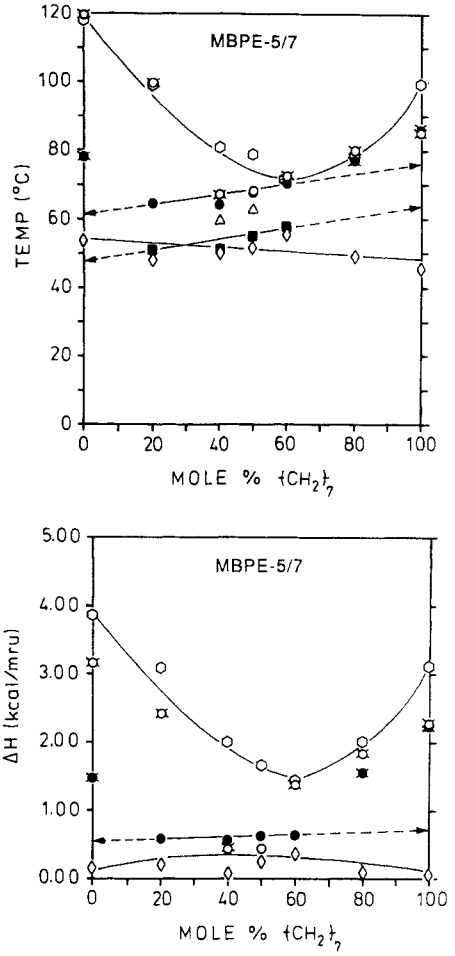

Figure 2. (a, top) Thermal transitions for homopolymers (MBPE-5 and MBPE-7) and copolymers [MBPE-5/7(A/B)]. First heating scan after high-temperature annealing [(○) T_{ki}]; first heating scan after room-temperature annealing [(○) T_{ki}, (○) T_{ni}, (△) T_{kk} or T_{kn}, (◇) T_{kk}]; and second heating scan [(●) T_{ki}, (●) T_{ni}, (■) T_{sn}]. Arrows point to virtual transitions for the homopolymers. (b, bottom) Enthalpy changes for homopolymers (MBPE-5 and MBPE-7) and copolymers [MBPE-5/7(A/B)]. First heating scan after high-temperature annealing [(○) ΔH_{ki}]; first heating scan after room-temperature annealing [(○) ΔH_{ki}, (○) ΔH_{ni}, (◇) ΔH_{kk}]; and second heating scan [(●) ΔH_{ki}, (●) ΔH_{ni}]. Arrows point to enthalpies of virtual transitions for the homopolymers.

heating scans. As we observe by comparing Figures 1a and 2a, copolymers MBPE-5/7(80/20) to MBPE-5/7(40/60) exhibit both nematic and smectic mesophases in the second heating scan (Table I). Nevertheless, annealing these copolymers at room temperature induces their crystallization. With the exception of MBPE-5/7(50/50), the melting temperatures of all other copolymers exceed the T_{s-n} and T_{n-i} transition temperatures determined from second heating scans. Therefore, the first scan after annealing at room temperature leads to a single copolymer exhibiting an enantiotropic nematic mesophase, i.e., MBPE-5/7(50/50). Annealing at higher temperatures for different durations (Figure 1b) leads to a shift of the melting temperatures above isotropization temperatures. Therefore, under these quasi-equilibrium conditions, all MBPE-5/7 copolymers exhibit only monotropic mesophases. Consequently, enantiotropic mesophases, which under equilibrium conditions are only monotropic, could be observed in the second heating scans. This behavior is certainly due to the highly depressed rate of crystallization of these copolymers. The phase diagrams from Figure 2 support our statement. In the second heating scans, we could not detect melting transitions for most of

the copolymers. This is due to their low rate of crystallization. However, after annealing, all copolymers crystallize, although their melting transition temperatures as well as their corresponding enthalpies are strongly depressed after copolymerization (Figure 2). We have to clearly mention that the melting transitions at high temperatures do not represent equilibrium values. The same is true for their corresponding thermodynamic parameters.

It is interesting to observe that, besides the high-temperature melting transitions, all polymers annealed at room temperature present melting transitions at low temperatures (Figure 1a, Table I). Contrary to the melting transitions displayed at high temperature, the melting transitions displayed at low temperature seem to be situated on a straight line when plotted as a function of copolymer composition (Figure 2a). The corresponding enthalpies are plotted in Figure 2b and with a certain amount of good will can be located on an upward curve which shows a maximum at about 50/50 composition. This is unexpected behavior for a crystalline phase. The only speculation we can make at the present time is that upon annealing at room temperature for the low-temperature crystalline phase the equilibrium state is reached more quickly in copolymers than in homopolymers. This is in contrast to the equilibrium situation of the high-temperature crystalline phase. Therefore, it seems that the rate of crystallization of the low-temperature crystalline phase is higher in copolymers. Simultaneously, the rate of crystallization of the high-temperature crystalline phase is lower in copolymers. Preliminary X-ray diffraction data have demonstrated that the low- and high-temperature transitions are indeed due to two different crystalline phases.[17] This behavior is consistent with the behavior of the other MBPE copolymers, and at the present time, we will not comment any further on the low-temperature crystalline phase.

DSC traces of the second heating scans and of the first heating scans after room-temperature and high-temperature annealings of the system MBPE-5/9 are presented in Figure 3. Table II summarizes all thermal transitions and thermodynamic parameters determined under different thermal histories.

First DSC heating scans after MBPE-5/9 polymer samples were annealed at room temperature, and first heating scans are similar. In comparison with the behavior of these polymers as resulted from second heating scans, when only the MBPE-5/9(20/80) copolymer and the two homopolymers were crystalline, after room-temperature annealation, all polymers have crystallized (Figure 3a, Table II). They exhibit a low-temperature melting transition which obeys a linear dependence versus copolymer composition (Figure 4a). The enthalpy changes associated with these transitions are plotted in Figure 4b, and they resemble the same behavior as the similar data for the copolymers MBPE-5/7. Upon annealing at room temperature, all polymers with the exception of MBPE-5/9-(50/50) and MBPE-5/9(40/60) also present melting transitions that exceed the isotropization transition temperatures. Upon annealing at high temperatures, all polymers give rise to melting transitions that occur at higher temperatures than their isotropization temperatures (Figure 3b). The melting transition temperatures and the corresponding thermodynamic parameters for the high melting transitions are plotted in Figure 4 and demonstrate a behavior that resembles the series of copolymers MBPE-5/7.

Figure 5a presents the first DSC heating scans of the room-temperature-annealed samples of the copolymers

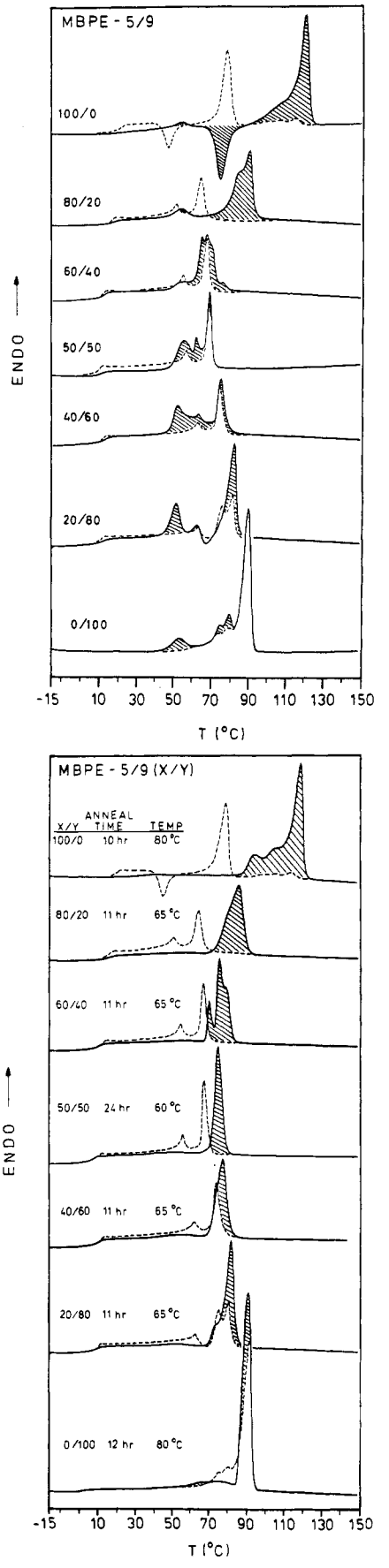

Figure 3. DSC thermograms of polyethers based on MBPE and 1,5-dibromopentane (MBPE-5), MBPE and 1,9-dibromononane (MBPE-9), and corresponding copolyethers [MBPE-5/9(A/B)]. (a, top) First heating scan after room-temperature annealing or first heating scan (—); second heating scan (- - -). (b, bottom) First heating scan after high-temperature annealing (—); second heating scan (- - -).

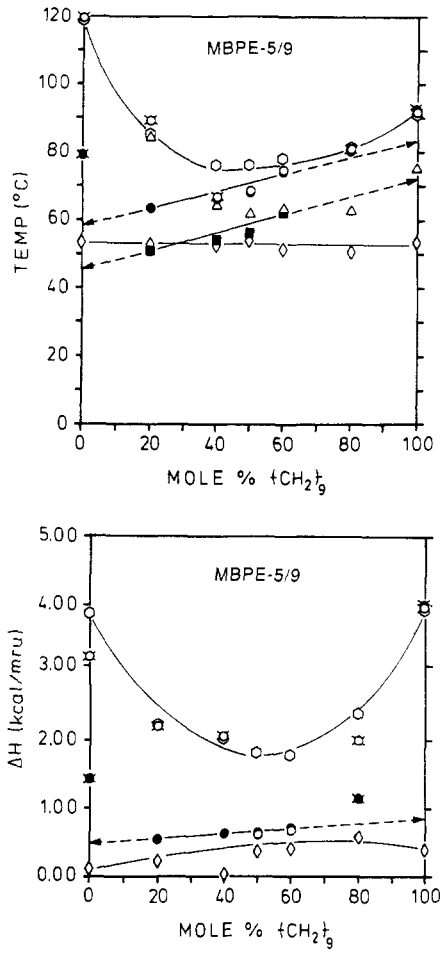

Figure 4. (a, top) Thermal transitions for homopolymers (MBPE-5 and MBPE-9) and copolymers [MBPE-5/9(*A*/*B*)]. First heating scan after high-temperature annealing [(○) T_{ki}]; first heating scan after room-temperature annealing [(○) T_{ki}, (○) T_{ni}, (△) T_{kk} or T_{kn}, (◇) T_{kk}]; and second heating scan [(●) T_{ki}, (●) T_{ni}, (■) T_{sn}]. Arrows point to virtual transitions for the homopolymers. (b, bottom) Enthalpy changes for homopolymers (MBPE-5 and MBPE-9) and copolymers [MBPE-5/9(*A*/*B*)]. First heating scan after high-temperature annealing [(○) ΔH_{ki}); first heating scan after room-temperature annealing [(○) ΔH_{ki}, (○) ΔH_{ni}, (◇) ΔH_{kk}]; and second heating scan [(●) ΔH_{ki}, (●) ΔH_{ni}]. Arrows point to enthalpies of virtual transitions for the homopolymers.

MBPE-5/11. All polymers display a melting transition situated below the smectic–nematic transition temperature. The high-temperature range of the DSC traces changes only for MBPE-5/11(100/0, 80/20, and 60/40). The other polymers do not change their high-temperature transitions upon annealing at room temperature. However, annealing at high temperatures induces the formation of a high-temperature crystalline phase in all polymers (Figure 5b). The low melting transitions located at low temperatures are all situated on a straight line (Figures 5a and 6a) and the enthalpy changes associated with these melting transitions are situated on an upward curve (Figure 6b). The melting transitions located at high temperatures and their corrresponding enthalpy changes are plotted in Figure 6 and exhibit the same trend as those of the two previous sets of copolymers. Comparing Figure 5a with Figures 3a and 1a, we can observe that only some of the copolymers based on these two highly dissimilar spacer lengths, i.e., MBPE-5/11(50/50) and MBPE-5/11(40/60), exhibit both smectic and nematic enantiotropic mesophases (Table III, Figure 6). This behavior may be derived from the higher rate of formation of the low-temperature crystalline phase, which, if formed in a large amount, retards the formation

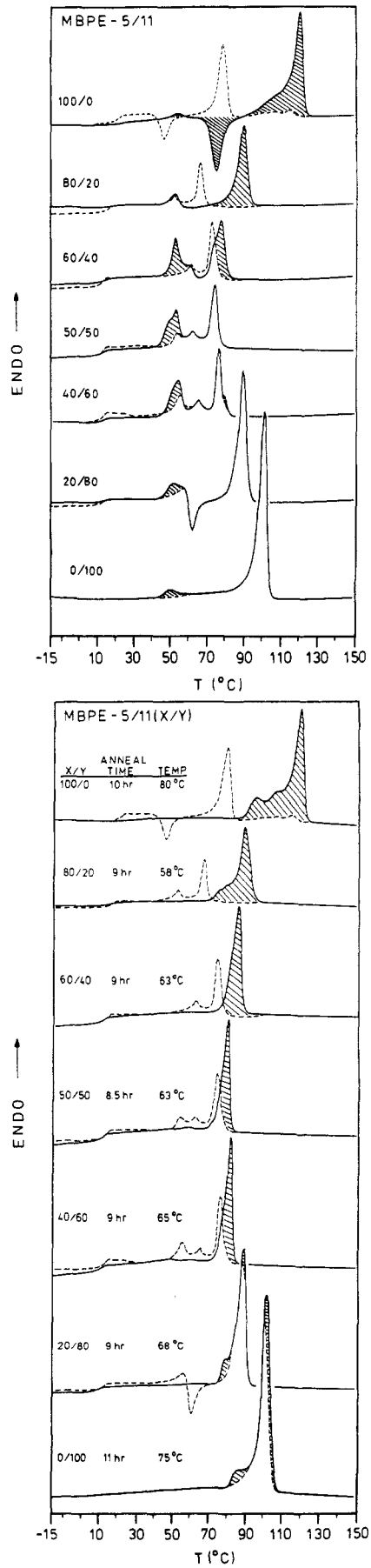

Figure 5. DSC thermograms of polyethers based on MBPE and 1,5-dibromopentane (MBPE-5), MBPE and 1,11-dibromoundecane (MBPE-11), and corresponding copolyethers [MBPE-5/11(*A*/*B*)]. (a, top) First heating scan after room-temperature annealing (—); second heating scan (- - -). (b, bottom) First heating scan after high-temperature annealing (—); second heating scan (- - -).

Table II
Characterization of Polyethers Based on MBPE and 1,5-Dibromopentane (MBPE-5) and 1,9-Dibromononane (MBPE-9) and of Corresponding Copolyethers [MBPE-5/9(*A*/*B*)] before and after Thermal Treatments

copolymer MBPE-5/9(*A*/*B*) 5/9 mole ratio	thermal transitions (°C) from DSC heating scans (20 °C/min) and corresponding enthalpy changes (kcal/mru) in parentheses		
	second heating scan	room-temp annealing	high-temp annealing
100/0	g 20 k 79 (1.44) k 115 (0.33) i	g 22 k 53 (0.12) k 120 (3.13) i	g 30 k 94 k 105 k 118 (3.87) i
80/20	g 15 s 51 (0.13) n 64 (0.54) i	g 18 k 53 (0.22) k 84 k 89 (2.21) i	g 16 k 85 (2.25) i
60/40	g 11 s 54 (0.15) n 66 (0.62) i	g 12 k 53 (0.05) k 64 k 67 k 76 (2.07[a]) i	g 11 k 70 k 76 k 79 (2.02[a]) i
50/50	g 9 s 56 (0.14) n 68 (0.67) i	g 11 k 54 (0.37) k 62 n 68 (0.61) i	g 8 k 76 (1.83) i
40/60	g 11 s 62 (0.13) n 74 (0.71) i	g 13 k 51 (0.41) s 63 n 75 (0.68) i	g 11 k 78 (1.80) i
20/80	g 9 k 62 k 74 n 80 (1.17[a]) i	g 12 k 50 (0.58) k 62 k 81 (2.00) i	g 9 k 81 (2.42) i
0/100	g 6 k 75 k 80 k 91 (4.02) i	k 53 (0.29) k 75 k 80 k 91 (3.93) i	g 3 k 91 (3.83) i

[a] Overlapping transitions.

Table III
Characterization of Polyethers Based on MBPE and 1,5-Dibromopentane (MBPE-5) and 1,11-Dibromoundecane (MBPE-11) and of Corresponding Copolyethers [MBPE-5/11(*A*/*B*)] before and after Thermal Treatments

copolymer MBPE-5/11(*A*/*B*) 5/11 mole ratio	thermal transitions (°C) from DSC heating scans (20 °C/min) and corresponding enthalpy changes (kcal/mru) in parentheses		
	second heating scan	room-temp annealing	high-temp annealing
100/0	g 20 k 79 (1.44) k 115 (0.33) i	g 22 k 53 (0.12) k 120 (3.13) i	g 30 k 94 k 105 k 118 (3.87) i
80/20	g 16 s 53 (0.10) n 66 (0.50) i	g 19 k 53 (0.20) k 89 (1.80) i	g 15 k 88 (2.18) i
60/40	g 12 s 61 (0.13) n 73 (0.75) i	g 14 k 53 (0.48) k 78 (1.41) i	g 11 k 83 (2.37) i
50/50	g 12 k 54 (0.10) s 62 (0.07) n 73 (0.86) i	g 13 k 53 (0.75) s 62 (0.07) n 74 (0.87) i	g 11 k 80 (2.08) i
40/60	g 12 k 55 (0.25) s 64 (0.08) n 75 (0.90) i	g 12 k 53 (0.80) s 62 (0.08) n 75 (0.94) i	g 11 k 80 (2.30) i
20/80	g 13 k 57 (0.41) k 89 (3.07) i	g 13 k 52 (0.75) k 89 (3.05) i	g 9 k 78 k 88 (3.63) i
0/100	g 5 k 101 (5.21) i	k 50 (0.18) k 100 (5.25) i	k 85 k 103 (6.00) i

Table IV
Characterization of Polyethers Based on MBPE and 1,7-Dibromoheptane (MBPE-7) and 1,9-Dibromononane (MBPE-9) and of Corresponding Copolyethers [MBPE-7/9(*A*/*B*)] before and after Thermal Treatments

copolymer MBPE-7/9(*A*/*B*) 7/9 mole ratio	thermal transitions (°C) from DSC heating scans (20 °C/min) and corresponding enthalpy changes (kcal/mru) in parentheses		
	second heating scan	room-temp annealing	high-temp annealing
100/0	g 7 k 85 (2.18) i	g 11 k 45 (0.06) k 85 (2.22) i	g 9 k 85 k 99 (3.12) i
80/20	g 11 k 62 (0.21) k 79 (1.91) i	g 12 k 49 (0.30) k 79 (1.87) i	g 10 k 80 (2.06) i
60/40	g 8 s 63 (0.14) n 75 (0.80) i	g 11 k 53 (0.43) k 68 (0.48) n 76 (0.68) i	g 9 k 63 k 73 (0.43) n 77 (1.38[a]) i
50/50	g 9 s 66 (0.15) n 78 (0.89) i	g 10 k 50 (0.30) k 60 (0.20) s 67 (0.06) n 79 (0.87) i	g 9 s 66 (0.15) k 70[b] (0.41) n 78 (0.89) i
40/60	g 8 s 65 (0.14) n 77 (0.89) i	g 9 k 49 (0.43) k 59 (0.43) s 65 (0.06) n 77 (0.90) i	g 8 s 65 (0.13) k 78 (1.34) i
20/80	g 9 k 50 (0.23) k 67 (0.06) k 82 (1.91) i	g 10 k 50 (0.56) k 64 (0.20) k 82 (1.93) i	g 7 k 82 (2.71) i
0/100	g 6 k 75 k 80 k 91 (4.02) i	k 53 (0.29) k 75 k 80 k 91 (3.93) i	g 3 k 91 (3.83) i

[a] Overlapping transitions. [b] Transition determined by successive annealings as shown in Figure 15.

of the higher temperature crystalline phase. This speculation is based on the difference between values of the enthalpy changes associated with the low-temperature crystalline phase plotted in Figures 6b, 4b, and 2b. As we can observe from these figures and Tables I–III, MBPE-5/11 copolymers exhibit higher enthalpy changes for this melting transition than copolymers MBPE-5/9 and MBPE-5/7. We believe that copolymers containing longer flexible spacers should display higher rates of crystallization than the other copolymers. This should be the case for both the low-temperature crystalline phases and for the high-temperature crystalline phases. However, due to a fast accumulation of a high degree of low-temperature crystalline phase, annealing below its melting point must suppress the rate of crystallization of the high-temperature crystalline phase. This assumption, if correct, is responsible for the phase behavior of the room-temperature-annealed samples of copolyethers containing even longer flexible spacers.

The phase behavior of the room-temperature-annealed samples of MBPE-7/9 copolymers can be observed from the DSC traces presented in Figure 7a. This set of copolymers represents the first one, which after annealing at room temperature in the first DSC heating scans crystalline melting transitions are observed only within the range of low temperatures. Even annealing at higher temperatures affects these copolymers phase behavior much less than any of the previous examples described thus far. This statement is based on the observation of the first heating scan obtained after polymer samples were annealed at high temperature (Figure 7b). The phase transition temperatures and the corresponding thermodynamic parameters for both sets of DSC traces are summarized in Table IV.

It is interesting to observe that MBPE-7/9(60/40) and MBPE-7/9(50/50) display enantiotropic nematic mesophases even after annealing at high temperatures (Figure 7b, Table IV). Repeated attempts to obtain a crystalline phase that will melt above the isotropization temperature for the MBPE-7/9(50/50) copolymer failed. A series of representative annealing experiments are presented in Figure 8. The most remarkable conclusion derived from the experiments presented in Figure 8 is that both the nematic–isotropic transition temperature and the corre-

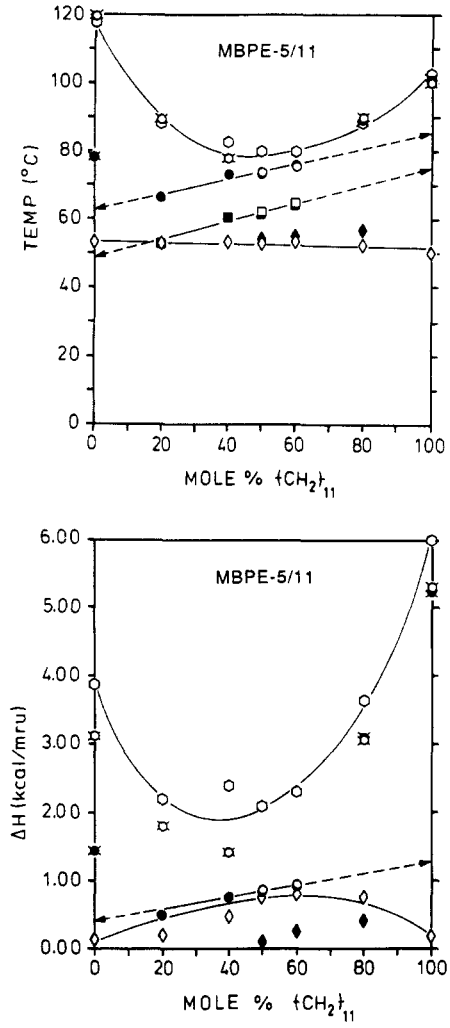

Figure 6. (a, top) Thermal transitions for homopolymers (MBPE-5 and MBPE-11) and copolymers [MBPE-5/11(A/B)]. First heating scan after high-temperature annealing [(○) T_{ki}]; first heating scan after room-temperature annealing [(○) T_{ki}, (○) T_{ni}, (□) T_{sn}, (◊) T_{kk} or T_{ks}]; and second heating scan [(●) T_{ki}, (●) T_{ni}, (■) T_{sn}, (♦) T_{ks} or T_{kk}]. Arrows point to virtual transitions for the homopolymers. (b, bottom) Enthalpy changes for homopolymers (MBPE-5 and MBPE-11) and copolymers [MBPE-5/11(A/B)]. First heating scan after high-temperature annealing [(○) ΔH_{ki}]; first heating scan after room-temperature annealing [(○) ΔH_{ki}, (○) ΔH_{ni}, (◊) ΔH_{kk} or ΔH_{ks}]; and second heating scan [(●) ΔH_{ki}, (●) ΔH_{ni}, (◊) ΔH_{ks}]. Arrows point to enthalpies of virtual transitions for the homopolymers.

sponding enthalpy change are not dependent on the thermal history of the sample. This demonstrates that the nematic–isotropic transition is thermodynamically controlled.

This result is in contrast to the behavior of polyethers and copolyethers based on 4,4′-dihydroxy-α-methylstilbene and flexible spacers containing an odd number of methylene units in their flexible spacer. These last polymers display kinetically controlled nematic–isotropic transitions.[15] The major difference between these two sets of copolymers is dissimilar rigidity of their mesogenic unit. In our opinion, it is not unexpected that a mesogenic unit like that derived from 4,4′-dihydroxy-α-methylstilbene, which upon polyetherification gives rigid constitutional isomeric structural units, has some difficulties in packing into the mesomorphic phase. Although after polyetherification the MBPE mesogenic unit group also gives constitutional isomeric structural units, its flexibility even in its anti conformer provides this extended flexible rodlike mesogenic group with the unique capability to accommo-

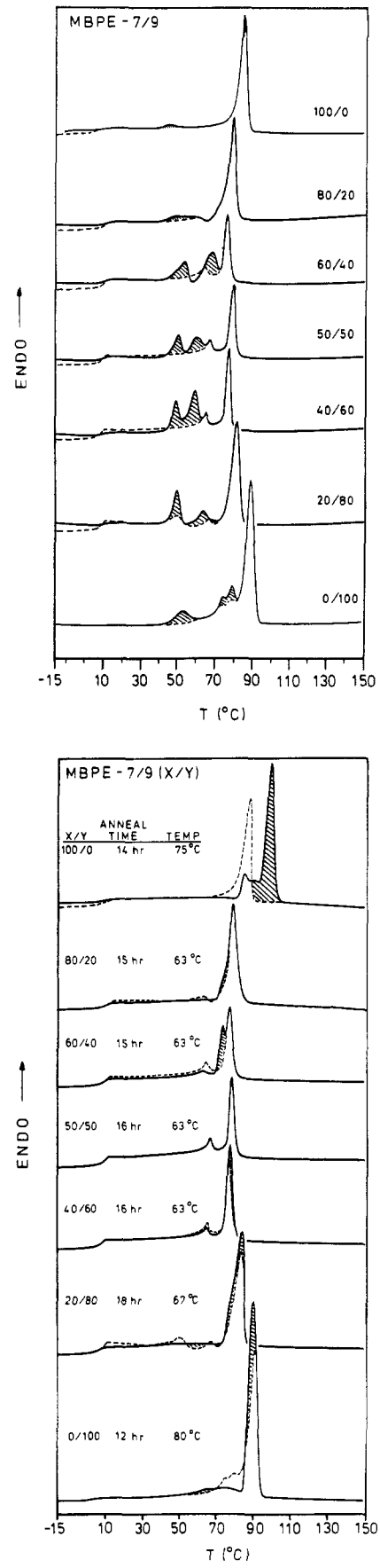

Figure 7. DSC thermograms of polyethers based on MBPE and 1,7-dibromoheptane (MBPE-7), MBPE and 1,9-dibromononane (MBPE-9), and corresponding copolyethers [MBPE-7/9(A/B)]. (a, top) First heating scan after room-temperature annealing (—); second heating scan (- - -). (b, bottom) First heating scan after high-temperature annealing (—); second heating scan (- - -).

Table V
Characterization of Polyethers Based on MBPE and 1,7-Dibromoheptane (MBPE-7) and 1,11-Dibromoundecane (MBPE-11) and of Corresponding Copolyethers [MBPE-7/11(*A*/*B*)] before and after Thermal Treatments

copolymer MBPE-7/11(*A*/*B*) 7/11 mole ratio	thermal transitions (°C) from DSC heating scans (20 °C/min) and corresponding enthalpy changes (kcal/mru) in parentheses		
	second heating scan	room-temp annealing	high-temp annealing
100/0	g 7 k 85 (2.18) i	g 11 k 45 (0.06) k 85 (2.22) i	g 9 k 85 k 99 (3.12) i
80/20	g 10 k 62 (0.13) k 79 (1.72) i	g 11 k 47 (0.58) k 57 k 78 (1.82) i	g 9 k 79 (2.07) i
60/40	g 10 s 69 (0.12) n 80 (0.87) i	g 9 k 52 (0.44) k 63 s 68 (0.28[a]) n 79 (0.84) i	g 9 k 68 k 82 (1.66) i
50/50	g 10 s 67 (0.13) n 77 (0.90) i	g 11 k 49 (0.43) k 58 s 67 (0.13) n 77 (0.88) i	g 9 5 65 k 80 (2.02) i
40/60	g 11 k 50 (0.09) s 69 (0.09) n 80 (1.06) i	g 10 k 47 (0.51) k 59 (0.13) s 68 n 79 (1.54) i	g 10 k 83 (2.26) i
20/80	g 13 k 49 (0.14) k 91 (3.30) i	g 13 k 47 (0.52) k 90 (3.33) i	g 10 k 90 (3.89) i
0/100	g 5 k 101 (5.21) i	k 50 (0.18) k 100 (5.25) i	k 85 k 103 (6.00) i

[a] Overlapping transitions.

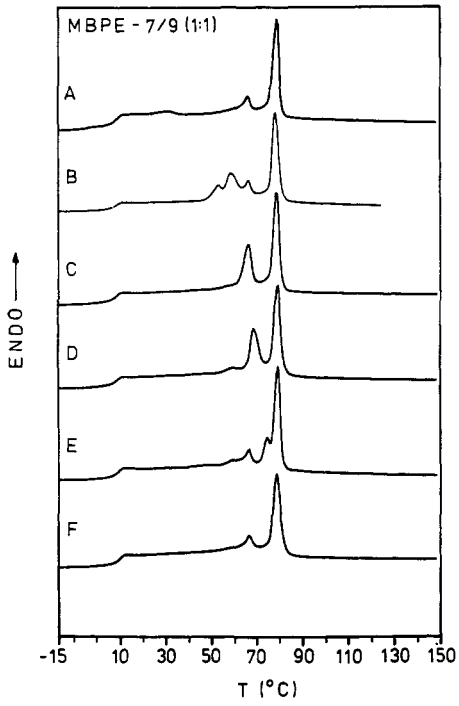

Figure 8. Representative DSC heating scans (20 °C/min) for copolyether MBPE-7/9(50/50) after different thermal treatments. (A) Quenched from isotropic melt into liquid nitrogen; (B) annealed at 40 °C for 2 h; (C) annealed at 55 °C for 2 h; (D) annealed at 55 °C for 2 h and then annealed at 60 °C for 10 h; (E) annealed at 55 °C for 2 h, at 60 °C for 10 h, and at 65 °C for 10 h; (F) annealed at 55 °C for 2 h, at 60 °C for 10 h, at 65 °C for 10 h, and at 70 °C for 10 h.

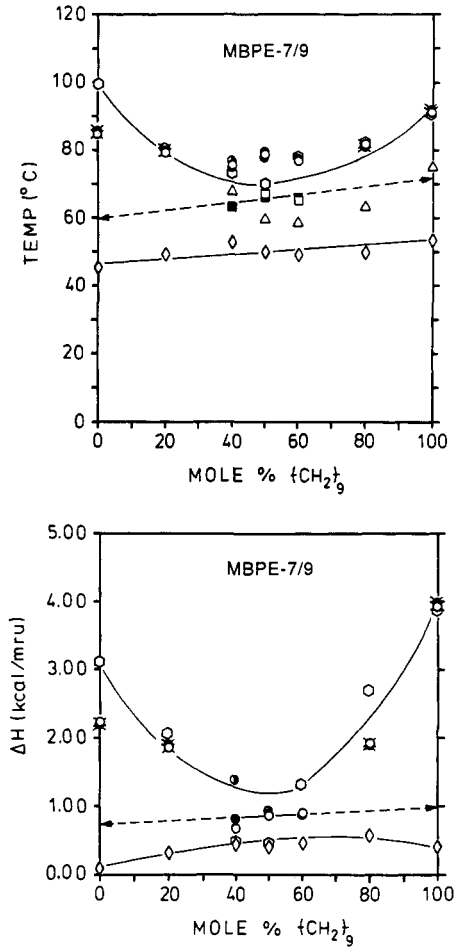

Figure 9. (a, top) Thermal transitions for homopolymers (MBPE-7 and MBPE-9) and copolymers [MBPE-7/9(*A*/*B*)]. First heating scan after high-temperature annealing [(○) T_{ki}, (◑) T_{ni}]; first heating scan after room-temperature annealing [(○) T_{ki}, (○) T_{ni}, (□) T_{sn}, (△) T_{ks}, T_{kk}, or T_{kn}, (◇) T_{kk}]; and second heating scan [(●) T_{ki}, (●) T_{ni}, and (■) T_{sn}]. Arrows point to virtual transitions for the homopolymers. (b, bottom) Enthalpy changes for homopolymers (MBPE-7 and MBPE-9) and copolymers [MBPE-7/9(*A*/*B*)]. First heating scan after high-temperature annealing [(○) ΔH_{ki}, (◑) ΔH_{ni}]; first heating scan after room-temperature annealing [(○) ΔH_{ki}, (○) ΔH_{ni}, (◇) ΔH_{kk}]; and second heating scan [(●) ΔH_{ki}, (●) ΔH_{ni}]. Arrows point to enthalpies of virtual transitions for the homopolymers.

date itself very quickly into a large variety of restricted environments.

The phase diagram for MBPE-7/9 copolymers is outlined in Figure 9a. The corresponding thermodynamic parameters are plotted in Figure 9b. The crystalline meltings from low temperatures (Figure 7a) are located again on a straight line (Figure 9a), and as in previous situations, the associated enthalpies of melting seem to provide an upward curvature with a maximum at about 50/50 ratio between the two spacers (Figure 9b). There is an additional melting transition located between the low-temperature one and the smectic mesophase (Figure 7a, Table IV). This transition temperature was plotted as a function of composition in Figure 9a and presents a dependence that is characteristic for a crystalline melting.

The first heating scan of the room-temperature-annealed samples of the series MBPE-7/11 resembles the behavior of the MBPE-7/9 copolymers. Their DSC traces are presented in Figure 10a. We see only melting transitions which are located below the smectic mesophase (Table V).

In addition, annealing at room temperature does not change the enantiotropic character of the nematic mesophase observed during the second heating scan in copolymers MBPE-7/11(60/40, 50/50, and 40/60). Annealing all these copolymers at higher temperatures induces a crystalline melting which appears at higher temperatures than the nematic–isotropic transition in all cases

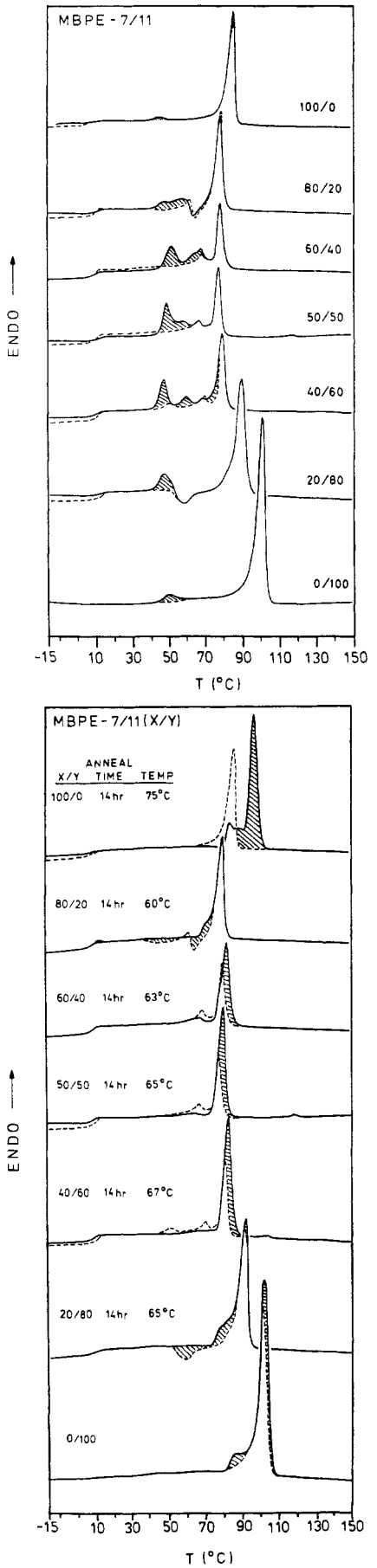

Figure 10. DSC thermograms of polyethers based on MBPE and 1,7-dibromoheptane (MBPE-7), MBPE and 1,11-dibromoundecane (MBPE-11), and corresponding copolyethers [MBPE-7/11(*A*/*B*)]. (a, top) First heating scan after room-temperature annealing (—); second heating scan (---). (b, bottom) First heating scan after high-temperature annealing (—); second heating scan (---).

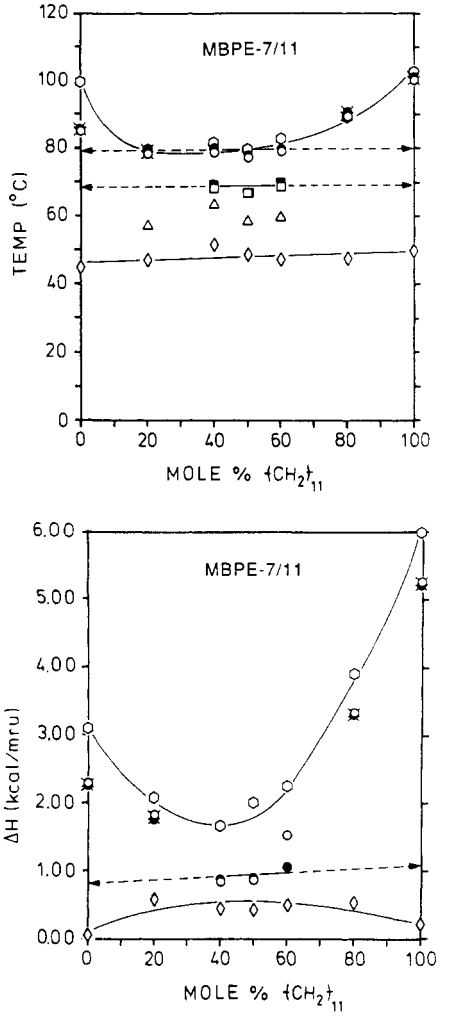

Figure 11. (a, top) Thermal transitions for homopolymers (MBPE-7 and MBPE-11) and copolymers [MBPE-7/11(*A*/*B*)]. First heating scan after high-temperature annealing [(○) T_{ki}]; first heating scan after room-temperature annealing [(○) T_{ki}, (○) T_{ni}, (□) T_{sn}, (△) T_{kk} or T_{ks}, (◇) T_{kk}]; and second heating scan [(●) T_{ki}, (●) T_{ni}, (■) T_{sn}]. Arrows point to virtual transitions for the homopolymers. (b, bottom) Enthalpy changes for homopolymers (MBPE-7 and MBPE-11) and copolymers [MBPE-7/11(*A*/*B*)]. First heating scan after high temperature annealing [(○) ΔH_{ki}]; first heating scan after room temperature annealing [(○) ΔH_{ki}, (○) ΔH_{ni}, (◇) ΔH_{kk}]; and second heating scan [(●) ΔH_{ki}, (●) ΔH_{ni}]. Arrows point to enthalpies of virtual transitions for the homopolymers.

(Figure 10b). Table V summarizes thermal transitions and thermodynamic parameters determined from both parts a and b of Figure 10. The phase diagram of thermal transitions is presented in Figure 11a, and the thermodynamic parameters are plotted in Figure 11b. The room-temperature annealing of MBPE-7/11 copolymers (Figure 10a) resembles the behavior of MBPE-7/9 copolymers (Figure 7a). However, the high-temperature annealing of MBPE-7/11 polymers resembles the behavior of MBPE-5/11, MBPE-5/7, and MBPE-5/9 copolymers (Figure 5b, 3b, and 1b).

The first heating DSC traces of the room-temperature-annealed MBPE-9/11 polymers are presented in Figure 12a together with the DSC traces of the second heating scans. This is the only set of copolymers that exhibits a sufficiently high rate of crystallization so that they display crystalline meltings for all copolymers even during the second and subsequent heating scans (Table VI, Figure 12a). Upon annealing at room temperature, we observe an enhancement of the enthalpy changes associated with the crystalline meltings already available from

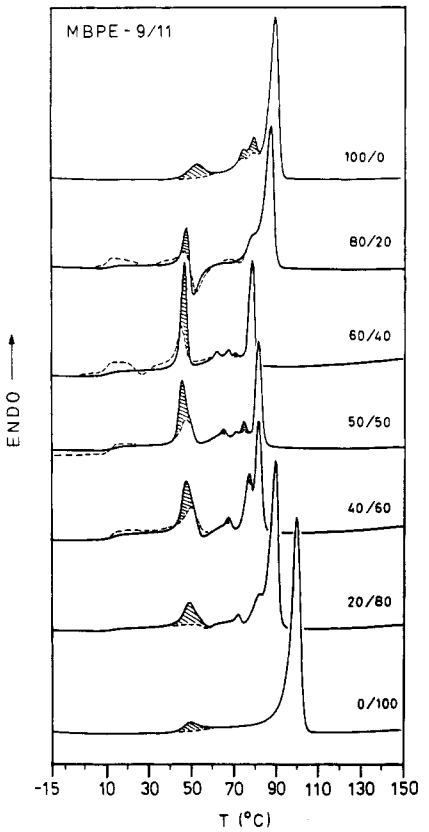

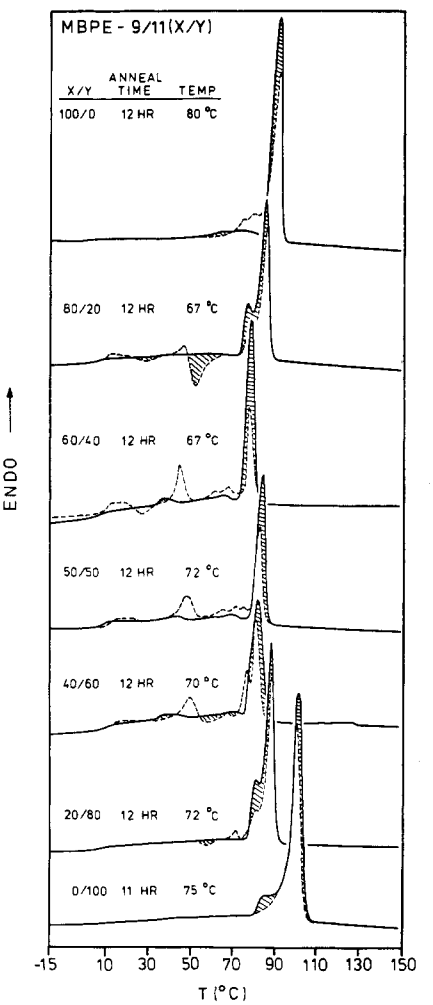

Figure 12. DSC thermograms of polyethers based on MBPE and 1,9-dibromononane (MBPE-9), MBPE and 1,11-dibromoundecane (MBPE-11), and corresponding copolyethers [MBPE-9/11(A/B)]. (a, top) First heating scan after room-temperature annealing (—); second heating scan (- - -). (b, bottom) First heating scan after high-temperature annealing (—); second heating scan (- - -).

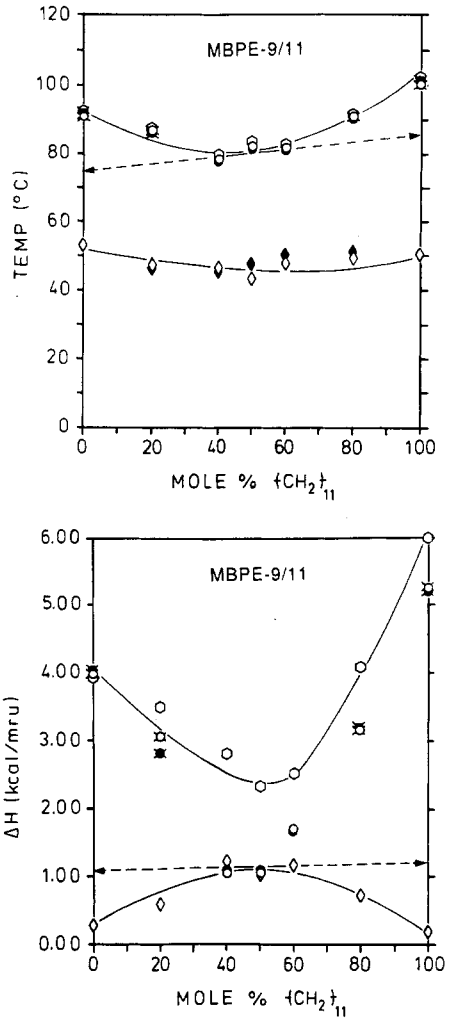

Figure 13. (a, top) Thermal transitions for homopolymers (MBPE-9 and MBPE-11) and copolymers [MBPE-9/11(A/B)]. First heating scan after high-temperature annealing [(○) T_{ki}]; first heating scan after room-temperature annealing [(○) T_{ki}, (○) T_{ni}, (◇) T_{kk}]; and second heating scan [(●) T_{ki}, (●) T_{ni}, (◆) T_{kk}]. Arrows point to virtual transitions for the homopolymers. (b, bottom) Enthalpy changes for homopolymers (MBPE-9 and MBPE-11) and copolymers [MBPE-9/11(A/B)]. First heating scan after high-temperature annealing [(○) ΔH_{ki}]; first heating scan after room-temperature annealing [(○) ΔH_{ki}, (○) ΔH_{ni}, (◇) ΔH_{kk}]; and second heating scan [(●) ΔH_{ki}, (●) ΔH_{ni}, (◆) ΔH_{kk}]. Arrows point to enthalpies of virtual transitions for the homopolymers.

the second heating scans (Figure 12a, Table VI). However, as in the case of MBPE-7/11 and MBPE-7/9 copolymers, no additional high-temperature melting transitions are observed after these samples were annealed at room temperature. Nevertheless, high-temperature annealing demonstrates that the enantiotropic mesophases determined from second heating scans are metastable and that in fact they are only monotropic (Figure 12b, Table VI). The thermal transitions from Figure 12 are plotted in Figure 13a, while the corresponding enthalpy changes are plotted in Figure 13b. Both sets of data resemble the behavior of the previously discussed sets of copolymers.

An inspection of the enthalpy changes associated with the nematic–isotropic transition and of the nematic–isotropic transition temperatures obtained before and after annealing (see all figures and tables from this manuscript) reveals that all polymers display thermodynamically controlled mesomorphic transitions.

Figure 14 presents a series of optical polarized micrographs obtained during the annealing of MBPE-7/9(50/50) for different durations at 70 °C. We can clearly observe

Table VI
Characterization of Polyethers Based on MBPE and 1,9-Dibromononane (MBPE-9) and 1,11-Dibromoundecane (MBPE-11) and of Corresponding Copolyethers [MBPE-9/11(*A*/*B*)] before and after Thermal Treatments

copolymer MBPE-9/11(*A*/*B*) 9/11 mole ratio	thermal transitions (°C) from DSC heating scans (20 °C/min) and corresponding enthalpy changes (kcal/mru) in parentheses		
	second heating scan	room-temp annealing	high-temp annealing
100/0	g 6 k 75 k 80 k 91 (4.02) i	k 53 (0.29) k 75 k 80 k 91 (3.93) i	g 3 k 91 (3.83) i
80/20	g 10 k 47 (0.30) k 77 k 86 (2.80) i	g 12 k 47 (0.58) k 78 k 87 (3.06) i	g 7 k 77 k 86 (3.52) i
60/40	g 10 k 45 (0.59) k 62 s 68 n 79 (1.08) i	g 11 k 46 (1.21) k 62 s 68 s 71 n (1.04) i	g 7 k 40 k 67 k 80 (2.83) i
50/50	g 12 k 47 (0.62) k 65 k 71 s 75 n 82 (1.08) i	g 13 k 43 (1.06) k 65 k 71 s 75 n 82 (1.05) i	g 8 k 44 k 69 k 84 (2.35) i
40/60	g 13 k 50 (0.77) k 68 k 77 n 82 (1.72[a]) i	g 13 k 48 (1.15) k 67 k 77 n 82 (1.75[a]) i	g 11 k 39 k 71 k 83 (2.54) i
20/80	g 11 k 52 (0.16) k 72 k 81 k 89 (3.19[a]) i	g 13 k 49 (0.71) k 72 k 81 k 89 (3.17[a]) i	g 7 k 89 (4.11) i
0/100	g 5 k 101 (5.21) i	k 50 (0.18) k 100 (5.25) i	k 85 k 103 (6.00) i

[a] Overlapping transitions.

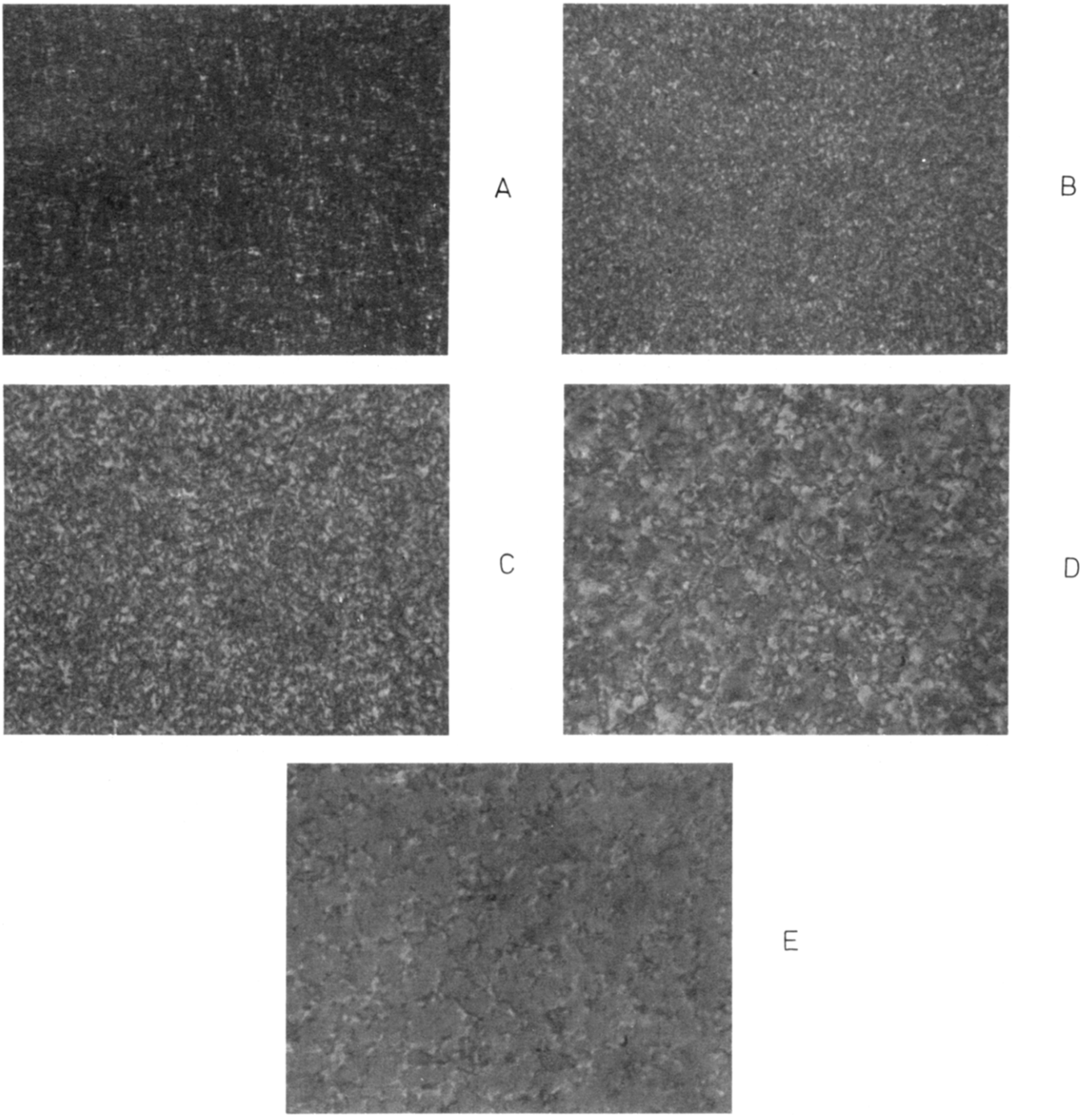

Figure 14. Optical polarized micrographs (magnification 130×) of MBPE-7/9(50/50) cooled from the isotropic phase to the nematic phase (70 °C) and annealed for various lengths of time: (A) 5 min; (B) 1 h; (C) 8 h; (D) 24 h; (E) 48 h.

a coarsening of the nematic texture. This coarsening may be related to the dynamics of disclinations.[15,18-20] However, as Figure 8 nicely demonstrates, the coarsening of this nematic texture is not accompanied by a change in the enthalpy change associated with the nematic–isotropic transition. This behavior is different from that of the similar polyethers and copolyethers based on 4,4′-dihydroxy-α-methylstilbene, which exhibit isotropization enthalpies dependent on the polymer thermal history.[15] This difference is, as already suggested, most probably dictated by the difference between the rigidity of these two mesogenic groups.

A different behavior can be observed in Figure 15, where some representative optical polarized micrographs are presented for sample MBPE-7/11(50/50). The crystallization of the polymer takes place within the nematic mesophase and gives rise to a biphasic system consisting of crystalline and nematic domains.

In conclusion, under equilibrium conditions, only the MBPE-7/9(50/50) and MBPE-7/9(60/40) copolymers display an enantiotropic nematic mesophase. The virtual enantiotropic or monotropic character of the mesophases of the other polymers and copolymers is determined by copolymer composition and thermal history of the sample. All copolymers and homopolymers exhibit at least two crystalline phases: one that melts at low temperatures (i.e., below the nematic–isotropic transition) and one that melts at high temperatures (i.e., above the nematic–isotropic transition). The rate of crystallization of each crystalline phase is dictated by the spacer length(s) and by copolymer composition. The longer the spacer length, the higher the rate of crystallization of both crystalline phases. As a general consequence, for copolymers based on shorter pairs of spacers, annealing at room temperature (i.e., above T_g but below the melting temperature of the first cyrstalline phase) induces the formation of small amounts of both crystalline phases. Subsequently, upon annealing at room temperature, most of the enantiotropic mesophases of the MBPE-5/7 and MBPE-5/9 copolymers become monotropic. The rate of crystallization of the other copolymers is much higher, and therefore, annealing at room temperature induces a higher content of low melting temperature crystalline phase. As a consequence, no higher melting temperature crystalline phase can be formed under these conditions, and therefore, annealing at room temperature maintains the enantiotropic mesophases for most copolymers. Annealing at higher temperatures (i.e., above the melting temperature of the lower crystalline phase) induces the formation of a high-temperature crystalline phase in all polymers. The only copolymers that do not give rise to a high melting temperature crystalline phase are MBPE-7/9(50/50) and MBPE-7/9(60/40), and therefore, they are the only copolymers displaying a thermodynamically stable enantiotropic mesophase. All this behavior is the result of the fact that crystalline phases are kinetically controlled and their rates of formation are highly depressed by copolymerization. At the same time, mesomorphic transitions are mainly thermodynamically controlled in both homopolymers and copolymers, and the rates of mesomorphic phase formation seem to be less affected by copolymerization. Therefore, the transformation of a virtual or monotropic mesophase into a enantiotropic one by copolymerization represents a kinetic effect. At the present time, we have no explanation for the unusual behavior of the MBPE-7/9(50/50) and MBPE-7/9(60/40) copolymers, which requires a quantitative understanding of the mechanism of crystallization of all these polymers.

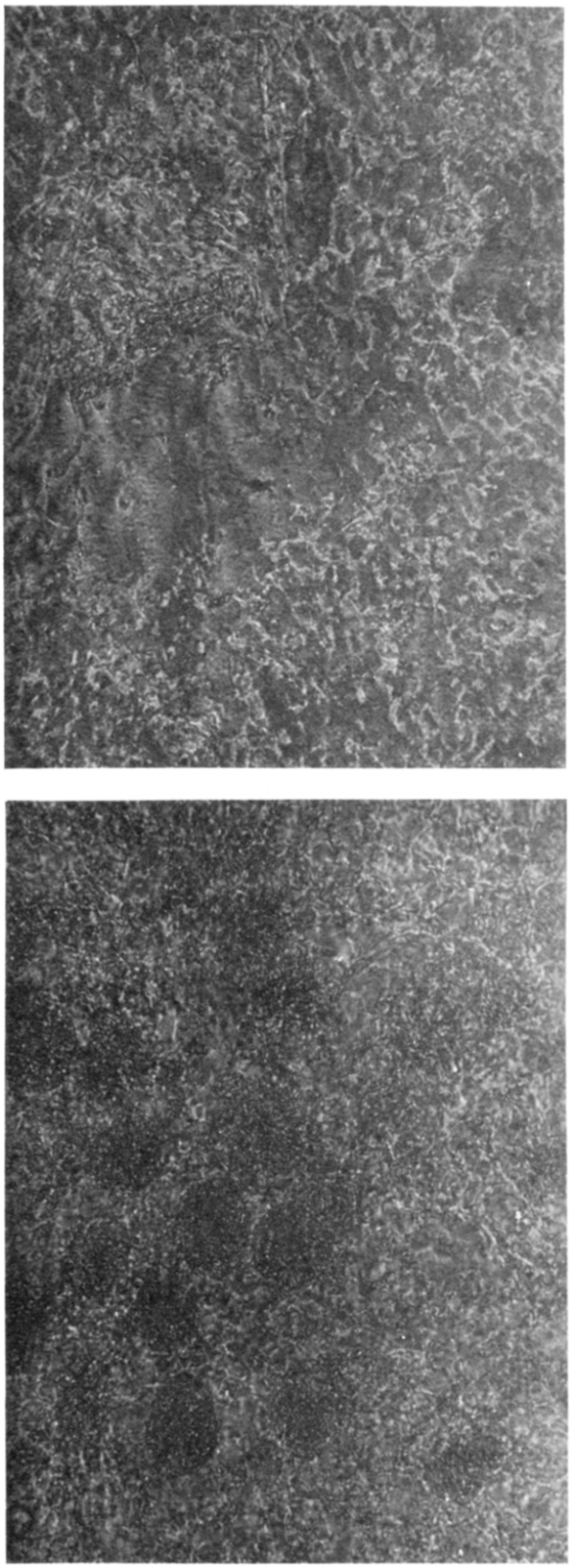

Figure 15. Optical polarized micrographs (magnification 125×) of MBPE-7/11(50/50): (A, top) cooled from the isotropic phase to the nematic phase (76 °C) and annealed for 20 h; (B, bottom) crystallites forming in the nematic phase after cooling from 76 to 68 °C and annealing for 26 h.

The determination of the crystalline phases of all these polymers is already in progress. Preliminary results show that all of them display similar crystalline phases as the corresponding polyethers and copolyethers based on 4,4′-dihydroxy-α-methylstilbene and an odd number of methylene units in the flexible spacer.[15]

Acknowledgment. Financial support of this work by the National Science Foundation, Polymers Program (DMR-86-19724), is gratefully acknowledged.

Registry No. MBPE-5 (copolymer), 115529-45-8; MBPE-7 (copolymer), 115529-46-9; MBPE-9 (copolymer), 115529-47-0; MBPE-11 (copolymer), 115529-48-1; MBPE-5/9 (copolymer), 117068-59-4; MBPE-5/7 (copolymer), 115529-49-2; MBPE-5/11 (copolymer), 117068-60-7; MBPE-7/9 (copolymer), 117068-61-8; MBPE-7/11 (copolymer), 117068-62-9; MBPE-9/11 (copolymer), 117068-63-0.

References and Notes

(1) Percec, V.; Yourd, R. *Macromolecules* **1988**, *21*, 3379.
(2) Percec, V.; Pugh, C. In *Side Chain Liquid Crystal Polymers*; McArdle, C. B., Ed.; Blackie: Glasgow, **1989**; p 30.
(3) Hsu, C. S.; Percec, V. *J. Polym. Sci., Part A: Polym. Chem.* **1987**, *25*, 2909.
(4) Percec, V.; Rodriguez-Parada, J. M.; Ericsson, C. *Polym. Bull. (Berlin)* **1987**, *17*, 347.
(5) Hsu, C. S.; Percec, V. *J. Polym. Sci., Part A: Polym. Chem.* **1989**, *27*, 453.
(6) Percec, V.; Yourd, R. *Macromolecules* **1989**, *22*, 524.
(7) Demus, D.; Richter, L. *Textures of Liquid Crystals*; Verlag Chemie: Weinheim, 1978.
(8) Ober, C. K.; Jin, J.; Lenz, R. W. *Adv. Polym. Sci.* **1984**, *59*, 130.
(9) Percec, V.; Nava, H. *J. Polym. Sci., Part A: Polym. Chem.* **1987**, *25*, 405.
(10) Blumstein, A.; Vilagar, S.; Ponrathram, S.; Clough, S. B.; Blumstein, R. *J. Polym. Sci., Part B: Polym. Phys.*, **1982**, *20*, 877.
(11) Roviello, A.; Santagata, S.; Sirigu, A. *Makromol. Chem., Rapid Commun.* **1984**, *5*, 209.
(12) Watanabe, J.; Krigbaum, W. R. *Macromolecules* **1984**, *17*, 2288.
(13) Amendola, E.; Carfagna, C.; Roviello, A.; Santogata, S.; Sirigu, A. *Makromol. Chem., Rapid Commun.* **1987**, *8*, 109.
(14) Fradet, A.; Heitz, W. *Makromol. Chem.* **1987**, *188*, 1233.
(15) Feijoo, J. L.; Ungar, G.; Owen, A. J.; Keller, A.; Percec, V. *Mol. Cryst. Liq. Cryst.* **1988**, *155*, 487.
(16) Percec, V.; Asami, K., unpublished data.
(17) Keller, A.; Ungar, G.; Yourd, R.; Percec, V., unpublished data.
(18) Frank, C. F. *Discuss. Faraday Soc.* **1958**, *25*, 19.
(19) Shiwaku, T.; Nakai, A.; Hasegawa, H.; Hashimoto, H. *Polym. Commun.* **1987**, *28*, 174.
(20) Rojstaezer, S.; Stein, R. S. *Mol. Cryst. Liq. Cryst.* **1988**, *157*, 293.

Nature of the Active Centers and the Propagation Mechanism of the Polymerization of β-Propiolactones Initiated by Potassium Anions

Zbigniew Jedliński* and Marek Kowalczuk

Institute of Polymer Chemistry, Polish Academy of Sciences, 41-800 Zabrze, Poland.
Received February 22, 1988; Revised Manuscript Received November 22, 1988

ABSTRACT: The chemical structure of the active centers formed during the polymerization of β-propiolactones initiated by potassium anions has been elucidated on the basis of the results of spectroscopic (^{1}H NMR, IR), chemical, and elemental analyses. In the initial step of propagation, two types of active species, carboxylate and alkoxide anions, are formed. The alkoxide anions disappear during the polymerization, and carboxylate anions are eventually the main propagation species.

Introduction

In our previous studies concerning the polymerization of β-propiolactones initiated by potassium anions, the formation of living polymers and also block polyesters was reported.[1,2] The proposed mechanism of ring opening involves in the initiation step the cleavage of the α carbon to β carbon bond in the monomer.[3,4] However, the propagation step of this polymerization has not been studied in detail.

New results concerning the nature of the active species in the polymerization of the β-propiolactones initiated by potassium anions are described in this paper.

Experimental Section

Materials. β-Propiolactone (**1**, from Fluka) was dried as described in ref 5 and distilled twice in an atmosphere of dry argon. The fraction boiling at 51 °C (10 mmHg) was collected. β-Butyrolactone (**2**, from Fluka) was dried in a similar manner. The fraction boiling at 47 °C (5 mmHg) was collected (99.8% GC). THF was purified as previously described[6] and was then distilled over a sodium–potassium alloy in an atmosphere of dry argon.

Preparation of the Initiator. A potassium solution rich in potassium anions was obtained by adding a THF solution of 18-crown-6 to a potassium mirror at 25 °C.[7] The concentration of potassium anions was taken as one-half of the total potassium concentration, as determined by the titration of the hydrolyzed sample with 0.03 N HCl.

Dimerization Reaction of β-Propiolactone (1) Initiated by Potassium Anions. The reaction was conducted in the apparatus described in ref 3. Into a potassium solution containing 0.004 mol of potassium anions, 0.576 g (0.008 mol) of β-propiolactone in 5 mL of dry THF was introduced under an argon atmosphere at a temperature of 25 °C. After 10 min, 2 g of acidic ion-exchange resin (Lewatit S 1080) were introduced into the reaction mixture (the resin was used as an acidification agent and also as 18-crown-6 adsorber). The solution was then filtered, the solvent was evaporated, and the product mixture was dried under high vaccum; yield 0.54 g (92%); IR (neat) ν_{max} = 3500, 3300, 2900, 1740, 1460, 1400, 1180, 1100 cm^{-1}. Elemental analysis for $C_6H_{10}O_4$: calcd C 49.31%, H 6.90%; found C 49.26%, H 7.02%. Molecular weight was 146 as determined by vapor pressure osmometry (VPO). The number of carboxyl end groups was equal to 0.60 and that of the hydroxyl end groups was equal to 0.42 per molecule of the product.

Polymerization of β-Lactones 1 and 2 Initiated by Potassium Anions. The polymerization experiments were conducted at a temperature of 25 °C as described previously.[3] The monomer concentration was equal to 0.4 mol/L in each experiment, and the concentration of potassium anions varied from 0.013 to 0.054 mol/L.

Measurements. The ^{1}H NMR spectra of the purified oligomers and polymers were run in $CDCl_3$ by using TMS as internal standard on either a Varian XL-100 or a Varian VXR-300 spectrometer.

The IR spectra were recorded on a Specord M80 Carl Zeiss Jena spectrophotometer.

Number-average molecular weights were determined by the VPO technique in $CHCl_3$ using a Knauer vapor pressure osmometer.

0024-9297/89/2222-3242$01.50/0